SERBIAN JOURNAL OF ELECTRICAL ENGINEERING
Vol. 17, No. 2, June 2020, 223-234

UDC: 621.313.323:004.4`416 **DOI: https://doi.org/10.2298/SJEE2002223N**

Optimization of Synchronous Reluctance Motor Based on Radial Basis Network

Amirhossein Erfani Nik[1], Jawad Faiz[1]

Abstract: This paper presents surrogate-model based optimization for synchronous reluctance motor (SynRm) with transversally laminated rotor. A radial basis function (RBF) model with 12 input variables and three outputs is first trained. A dataset is obtained using finite element method to estimate parameters of RBF model. By building RBF model, the RBF network can predicts the outputs of the SynRm with good accuracy Using non-dominated sorting genetic algorithm (NSGA II), pareto front is obtained. The SynRm is designed to maximize the maximum developed torque and power factor of the motor with constrained torque ripple.

Keywords: Electrical machine design, Synchronous reluctance motor, Multi-objective optimizations, Surrogate-model.

1 Introduction

The synchronous reluctance motor (SynRm) has been received much attention in recent years. In comparison with induction motor, as a widely used motor in the industry, the SynRm has less copper loss and as a result its efficiency is higher than induction motor that meets ultra-premium efficiency (IE5) class [1]. Due to the lack of copper loss in the rotor of SynRm, the rotor temperature is lower, therefore, its reliability is better [2]. It has higher power and torque density [3]. The overload capability of this motor is also greater than induction motor [4]. In addition, the lack of a rare earth permanent magnet (PM) in the structure of the SynRm compared to PM machines is an advantage for this motor leading to a lower cost [2].

Optimization is an important part of any engineering design. The design of electric machines is no exception. The design of electric machines can be divided into two parts: sizing and optimization. This paper deals with latter part for the SynRm. The purpose of the optimization is to obtain the best possible

---

An earlier version of this paper was presented at the 14th International Conference on Applied Electromagnetics – PES 2019, Niš, Serbia.

[1]Centre of Excellent on Applied Electromagnetic Systems, School of Electrical and Computer Engineering, College of Engineering, University of Tehran, North Karagar Avenue, Tehran 1439957131, Iran E-mails: amirerfani@ut.ac.ir; jfaiz@ut.ac.ir

design according to the design goals in electric machine. If optimization involves more than one objective, the goal is to find a non-dominant solution. Under these circumstances, the objective may also conflict with each other, depending on the application of motor, one of these solutions is selected as the final design [5].

Optimization algorithms are iterative process and, in each iteration, objective function is evaluated. In electrical machines optimization with more than one objective, many objective functions are evaluated. Two to four Objectives can reach 25,000 to 150,000 objective function evaluations [5]. Increasing the decision variables also leads to an increase in the objective function evaluation to achieve desirable results [6].

In electric machines, the objective function is mainly evaluated by the finite element method (FEM) for each iteration of optimization algorithms [7]. The FEM is a time-consuming technique, however, in optimization process, generally small set of decision variables and objectives are chosen. Also, considering stochastic nature of heuristic optimization algorithms, there is need to run multiple heuristic algorithms to achieve reliable pareto front [8].

Rotor structure of the SynRm has many geometrical variables that affect the outputs such as torque, torque ripple, power factor and efficiency [9]. Therefore, the motor needs to be optimized to achieve acceptable performance.

Alternative method for function evaluation is to make surrogate model that represents an original model in simplified form. Based on samples that obtained from design of experiment (DOE), a model is developed that maps inputs vector to output [10]. In recent years, this method has attracted more attention in the optimization of electric machines. Some popular surrogate models are response surface methodology (RSM) [1], artificial neural networks (ANN) [11] and box-behnken design [12].

This paper presents the RBF model to interpolate behavior of the SynRm. The goal is to achieve the maximum torque and maximum power factor having torque ripple constraint. Non-dominated sorting genetic algorithm (NSGA II), that uses RBF model for evaluation objective function, is used.

2 Design Space Exploration

Fig. 1 shows the initial SynRm and its selected input variables. Initial sizing is based on [13]. **Table 1** summarizes the characteristics of the proposed motor. To obtain minimum torque ripple and low distortion of the air gap magnetic field, rotor has three barrier and stator has 36 slot with 2 layers of winding [14].

The purpose of introducing surrogate model is to learn mapping $y = f(x)$ from collected input vector $\boldsymbol{X}$ and scaler output y. This dataset can be obtained from physical experiment or computer simulation. Surrogate model requires the output values $y(n)$ that obtained from $X(n)$ to approach the best approximation for the system. A well-posed model requires sample points that represent whole design space. In the design of experiment, purpose of sampling plan is selected points to acquire maximum information in search space. The DOE full factorial technique has been used to sample the design space to develop accurate surrogate model. However, this method has high cost FEM simulation [15]. For example, in problem with 5 parameters and 10-level full factorial, 100000 FEM simulations are needed. Latin hyper cube sampling is another DOE technique which can be used. Important feature of this sampling plan is uniform coverage of the design space using space-filling criteria [15].

Table 1
Motor parameters.

Parameter	Value	Parameter	Value
Power (kW)	2.2	Rotor diameter (mm)	118
Poles	4	Air gap (mm)	1
Speed (rpm)	1500	Turn	324
DC-link	600	Current (A)	6.57

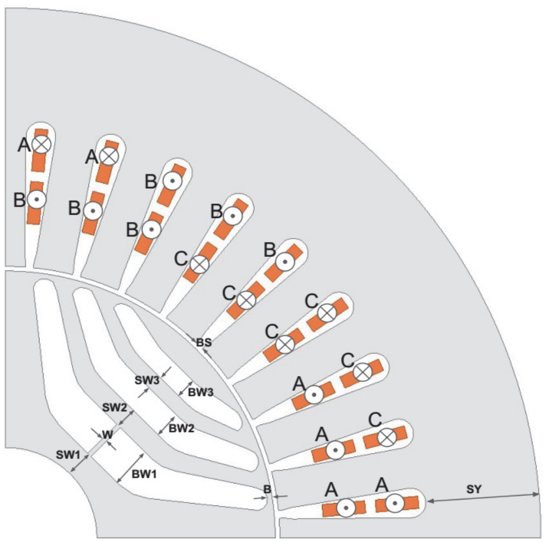

Fig. 1 – *Structure of motor and selected input variables.*

For the input points in the sampling plan, the output variables acquired from the FEM. In optimization process, the average torque (T_{avg}) and power factor (pf) are selected as output variables and torque ripple (T_{ripple}) as constraint. Low power factor is one of the disadvantages of the SynRm and low power factor causes higher cost for the drive of the motor. T_{avg}, (T_{ripple}) and pf are calculated as fallow [3]:

$$T_{avg} = \frac{1}{2\pi}\int_0^{2\pi} T_m(\vartheta_m)d\vartheta_m\,, \tag{1}$$

$$T_{ripple} = \frac{\max[T_m(\vartheta_m)] - \min[T_m(\vartheta_m)]}{T_{avg}}\,, \tag{2}$$

$$pf = \frac{V_d I_d + V_q I_q}{VI}\,. \tag{3}$$

Table 2 specifies the boundary of the design space**.** Limitation of barriers is imposed by geometry feasibility. To optimize motor with maximum torque per current strategy, current angle is selected as variable in the design space.

Table 2
Design space.

Variable	Range	Variable	Range
BW1 (mm)	4-9	W (mm)	1-3
BW2 (mm)	3-6	B (mm)	1-3
BW3 (mm)	1-4	BS (mm)	1.5-3
SW1 (mm)	0.8-6.9	SY (mm)	15-25
SW2 (mm)	0.6-4.6	Lstk (mm)	50-70
SW3 (mm)	0.2-2.85	Current angle	40-80

For the entire design space 12 variables are sampled using Latin hypercube [16]. For all samples, it has been ensured that instances not violated geometric limitations. 2992 instances obtain from sampling procedure. These instances represent entire design space uniformly. Fig. 2 shows the distribution of the average torque, power factor and torque ripple.

Fig. 3 shows that most of the output is gathered in non-desirable points. Another way is to visualize the output and show correlation between the output using scatter plot. In Fig. 4 radius and color represent power factor. This figure shows torque and torque ripple are not much correlated. Also, acceptable power factor can be achieved. Therefore to have acceptable outputs, there is need to search whole design space with optimization algorithms.

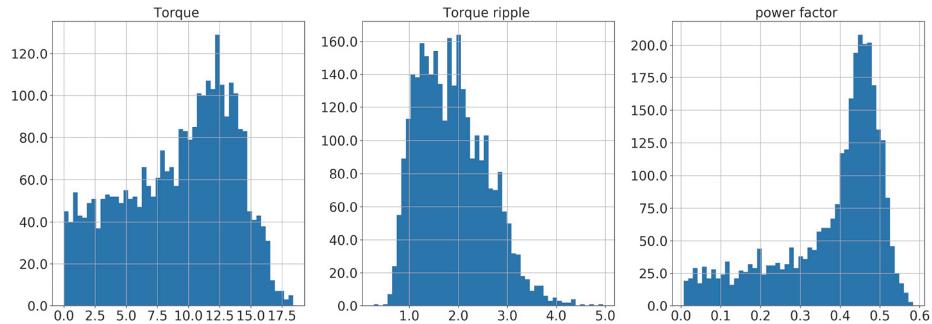

Fig. 2 - *Distribution of torque and torque ripple and power factor in design space.*

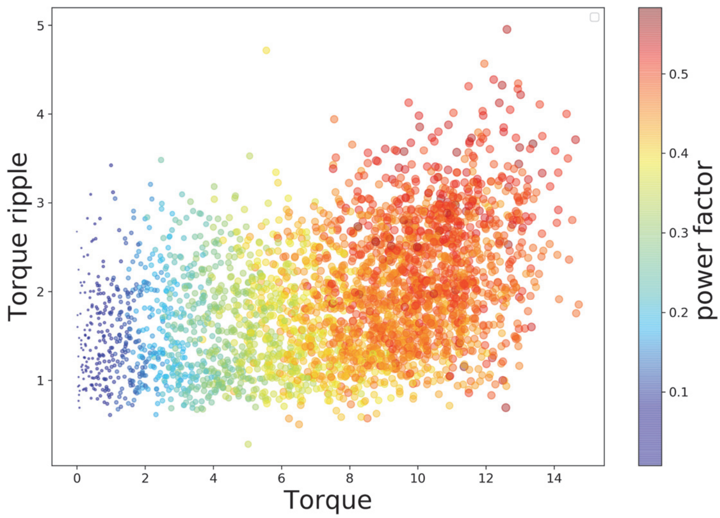

Fig. 4 – *Scatter plot of output variables.*

3 RBF Model Approximation

After creating sampling space, a relationship between

$$X = \{x_1, x_2, \ldots\ldots, x_n \mid x_i \in R^D\}$$

and its corresponding output

$$Y = \{y_1, y_2, \ldots\ldots, y_n \mid y_i \in R^q\}$$

must be found. This relationship is found using the radial basis function network. The RBF is an empirical approach to determine the relation of the input and output variables and shorten optimization time dramatically. This model is capable to approximate the nonlinear behavior. The analytical relationship of the RBF is as follows [17]:

$$f(x)=\sum_{j=1}^{n}\beta_j H\left(\left\|x-x_j\right\|\right), \tag{4}$$

where x_j is the center points of the RBF network, which is equal to the points of the sample space. $\left\|x-x_j\right\|$ is the norm or the distance of the input point with the center points. β_j are the unknown coefficients of the RBF network, to be obtained in the training process using the sample space. $H(r)$ indicates the basis function. In electromagnetic applications, basis functions usually are guessed multi-quadrics (MQ) and inverse multi-quadrics (IMQ). These basis functions are as follows:

$$\text{Gauss: } H(r)=\exp(-c^2r^2), \tag{5}$$

$$\text{MQ: } H(r)=\exp(r^2+c^2)^{1/2}, \tag{6}$$

$$\text{IMQ: } H(r)=\exp(r^2+c^2)^{-1/2}. \tag{7}$$

To train this network using the sample space, each sample distance from all other center points is calculated. So, the following matrix is obtained.

$$\begin{bmatrix} H\left(\left\|x_1-x_1\right\|\right) & H\left(\left\|x_1-x_2\right\|\right) & \cdots & H\left(\left\|x_1-x_n\right\|\right) \\ H\left(\left\|x_2-x_1\right\|\right) & H\left(\left\|x_2-x_2\right\|\right) & \cdots & H\left(\left\|x_2-x_n\right\|\right) \\ \vdots & \vdots & \ddots & \vdots \\ H\left(\left\|x_n-x_1\right\|\right) & H\left(\left\|x_n-x_2\right\|\right) & & H\left(\left\|x_n-x_n\right\|\right) \end{bmatrix} \begin{bmatrix} \beta_1 \\ \beta_2 \\ \vdots \\ \beta_n \end{bmatrix} = \begin{bmatrix} y_1 \\ y_2 \\ \vdots \\ y_n \end{bmatrix}. \tag{8}$$

It is clear that although the RBF network is nonlinear, finding its coefficients turns into a linear relationship. So, the coefficients are determined as follows.

$$\beta=\boldsymbol{H}^{-1}\boldsymbol{y}. \tag{9}$$

If any of the basis functions are used, the unknown variable c must be specified during the training. Training RBF network means determining parameter as such that the model fits training set. A criterion is needed for this purpose to measure how well the model fit training data. The most common criterion for regression is root mean square error (RMSE) shown in (10) [18]. For training the RBF network, the goal is finding the parameter that minimizes the RMSE:

$$RMSE=\sqrt{\frac{1}{m}\sum_{i=1}^{m}(H(x^{(i)})\beta-y^{(i)})}. \tag{10}$$

Before starting training procedure, 15% of the dataset is set aside. This is crucial for training any surrogate model to estimate generalization error of model to new inputs [18]. This test set must not be participated in the training procedure and only used after training model and tweaking its parameter to evaluate the final model for the new input.

To determine c in the basis function, cross validation is used. Cross validation involves splitting the training set into k-fold and training the model k times with k-1 subset and validating its output; based criteria is chosen, with remaining subset.

Surrogate models do not perform well if the inputs have very different scales. So, for feature scaling is most import transformation that must be applied to the inputs of the data set. There are two common ways for the scaling features of min-max scaling and standardization [18]. Here, the min-max scaling is used and the input data are mapped between 0 to 1 based on the following equation:

$$normalize(x) = \frac{x - \min(x)}{\max(x) - \min(x)} . \tag{10}$$

In the RBF training, Gaussian basis is selected. With grid search and cross validation score, constant c of kernel basis is found for the average torque, power factor and torque ripple separately. For new points, using (4) for prediction takes 0.012s with Intel core-i7 4700Hq. This time for the FEM simulation is 139 s.

Fig. 5 shows the outputs obtained from FEM versus values predicted by the RBF model. There is a good agreement between the FEM and the RBF model prediction at the test points. The RMSE for torque prediction in the test set is 0.1397, for torque ripple prediction is 0.2536 and for power factor is 0.1107.

4 Motor Optimization with Surrogate Model

To search design space for optimum design, the NSGA II is used. On contrary to the single objective problem, in multi-objective optimization, space of object is not sortable. In the NSGA II, domination and crowding distance is used for selecting of solution [19].

Objectives of optimization are maximizing average torque and power factor with constraint of torque ripple. In each function evaluation, if peak to peak torque ripple is more than 2 Nm, penalty is considered for that position.

Fig. 6 shows the flow-chart of the optimization, based on the RBF network that is a surrogate model.

In optimization procedure, number of function evaluations to achieve optimum position is 60000 in each run of the NSGA II. Each iteration of the NSGA II, that involves 300 function evaluations, lasts 18.75 s. This shows the advantage of the RBF model. Fig. 7 shows the pareto front that has been obtained from the NSGA II.

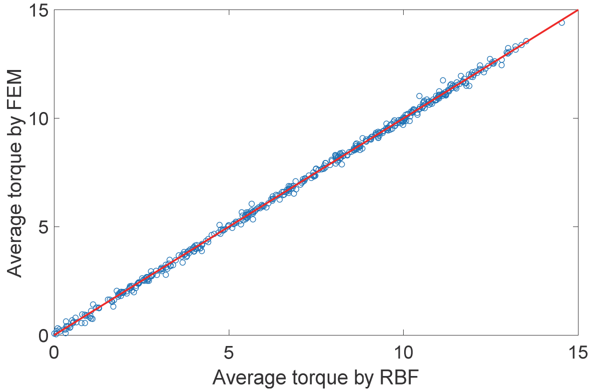

(a)

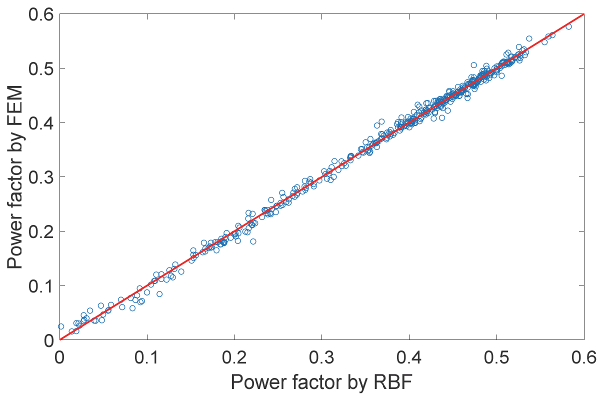

(b)

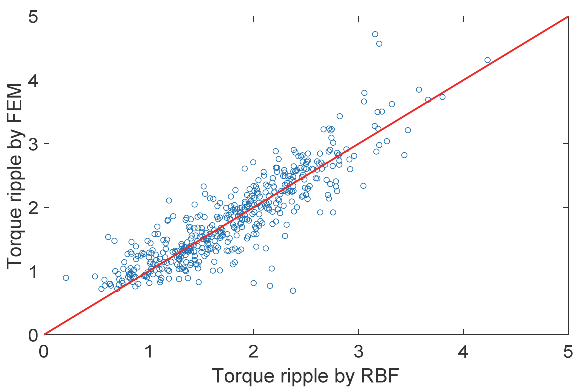

(c)

Fig. 5 – *FEM versus prediction of RBF model:*
(a) *average torque;* (b) *power factor;* (c) *torque ripple.*

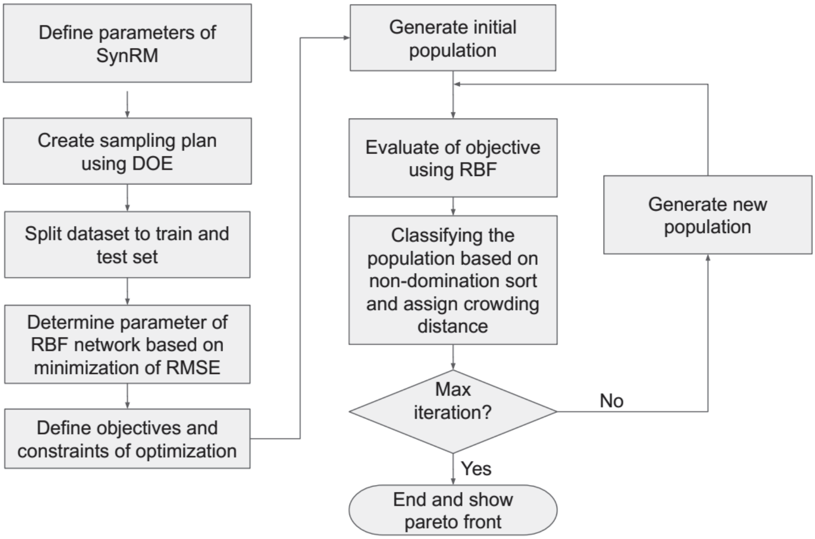

Fig. 6 – *Surrogate based optimization flow-chart of SynRm.*

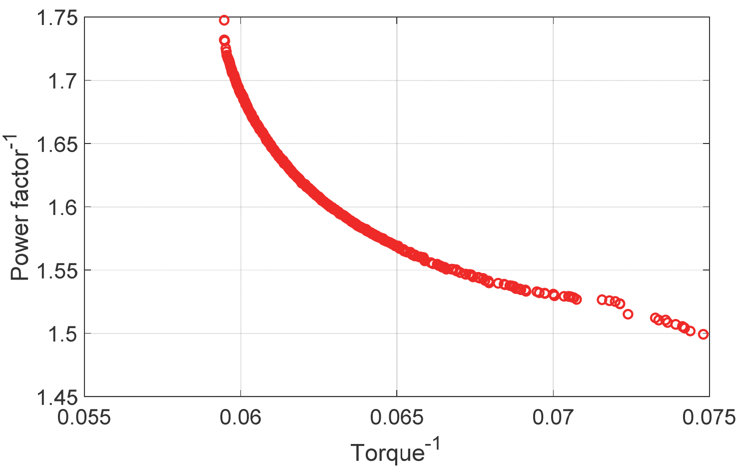

Fig. 7 – *Pareto front.*

To evaluate the output of the optimization process, the optimum motor, selected from the pareto front, is simulated using the FEM. **Table 3** summarizes the comparison between the outputs of the RBF and FEM. According to this table, there is a good agreement between the surrogate model and the FEM model. Fig. 8 shows the torque of the selected point from the pareto front, obtained from the FEM. The optimized motor efficiency is 91.2%. Fig. 9 presents the flux density and flux path.

Table 3
Comparison of FEA and RBF at optimum point.

	Average torque (Nm)	Torque ripple (%)	Power factor
FEM	15.92	10.17	0.60
RBF	15.73	7.62	0.61

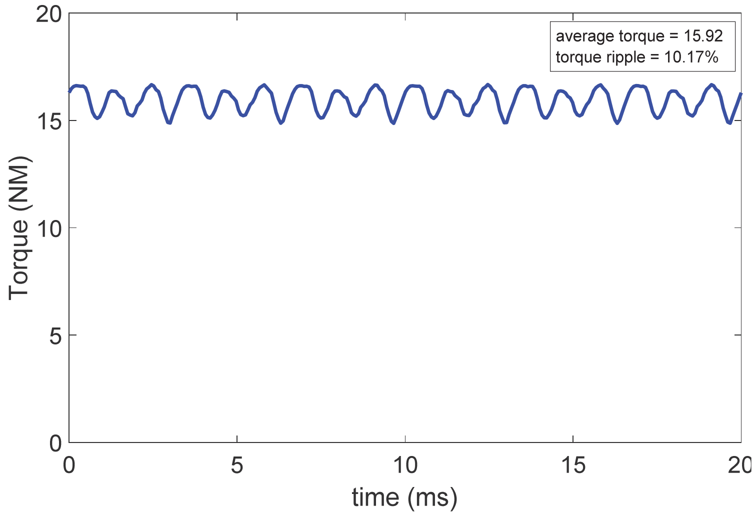

Fig. 8 – *Output torque of selected design from pareto front.*

5 Conclusion

This paper presents the design and optimization of a synchronous reluctance motor. Due to computational burden of the FEM, the RBF surrogate model was used in optimization process. The RBF model was tested to validate the accuracy of the result with the test samples. With validation with test, the guarantied model can predict a new input that not participate in training procedure. In optimization process, the NSGA II algorithm was integrated with the RBF and the pareto front was reported. Advantage of using the NSGA II is that the multi-objective algorithm does not need to be specify weight of each objective. Finally, the optimum point selected from the pareto front, was simulated with the FEM and the outputs were compared with the outputs of the RBF and a good agreement was achieved.

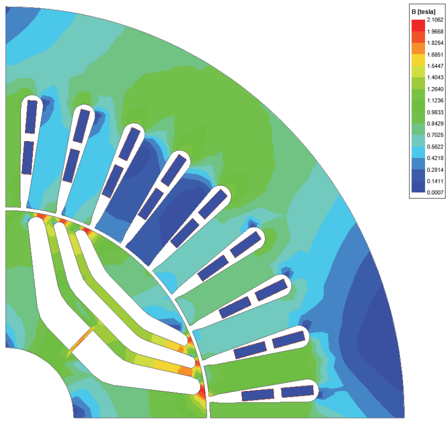

(a)

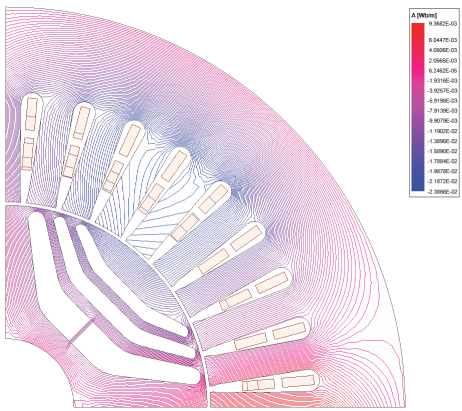

(b)

Fig. 9 – (a) *Flux density distribution;* (b) *Flux paths.*

6 References

[1] D.- H. Jung, Y. Kwak, J. Lee, C.- S. Jin: Study on the Optimal Design of PMa-SynRM Loading Ratio for Achievement of Ultrapremium Efficiency, IEEE Transactions on Magnetics, Vol. 53, No. 6, June 2017, pp. 1 – 4.

[2] G. Pellegrino, T.M. Jahns, N. Bianchi, W. L. Soong, F. Cupertino: The Rediscovery of Synchronous Reluctance and Ferrite Permanent Magnet Motors: Tutorial Course Notes, 1st Edition, Springer, Basel, 2016.

[3] M. Di Nardo, G. Lo Calzo, M. Galea, C. Gerada: Design Optimization of a High-Speed Synchronous Reluctance Machine, IEEE Transactions on Industry Applications, Vol. 54, No. 1, February 2018, pp. 233 – 243.

[4] G. Pellegrino, A. Vagati, B. Boazzo, P. Guglielmi: Comparison of Induction and PM Synchronous Motor Drives for EV Application Including Design Examples, IEEE Transactions on Industry Applications, Vol. 48, No. 6, December 2012, pp. 2322 – 2332.

[5] R.C.P. Silva, T. Rahman, M.H. Mohammadi, D.A. Lowther: Multiple Operating Points Based Optimization: Application to Fractional Slot Concentrated Winding Electric Motors, IEEE Transactions on Industrial Electronics, Vol. 65, No. 2, February 2018, pp. 1719–1727.

[6] Q. Zhang, H. Li: MOEA/D: A Multiobjective Evolutionary Algorithm based on Decomposition, IEEE Transactions on Evolutionary Computation, Vol. 11, No. 6, December 2007, pp. 712 – 731.

[7] A. Cavagnino, G. Bramerdorfer, J.A. Tapia: Optimization of Electric Machine Designs-Part II, IEEE Transactions on Industrial Electronics, Vol. 65, No. 2, February 2018, pp. 1700 – 1703.

[8] G. Pellegrino, F. Cupertino, C. Gerada: Automatic Design of Synchronous Reluctance Motors focusing on Barrier Shape Optimization, IEEE Transactions on Industry Applications Vol. 51, No. 2, April 2015, pp. 1465 – 1474.

[9] R.- R. Moghaddam, F. Gyllensten: Novel High-Performance SynRM Design Method: An Easy Approach for a Complicated Rotor Topology, IEEE Transactions on Industrial Electronics, Vol. 61, No. 9, September 2014, pp. 5058 – 5065.

[10] G. Bramerdorfer, J.A. Tapia, J.J. Pyrhönen, A. Cavagnino: Modern Electrical Machine Design Optimization: Techniques, Trends, and Best Practices, IEEE Transactions on Industrial Electronics, Vol. 65, No. 10, October 2018, pp. 7672 – 7684.

[11] A. Fatemi, D.M. Ionel, N.A.O. Demerdash, S. J. Stretz, T. M. Jahns: RSM-DE-ANN Method for Sensitivity Analysis of Active Material Cost in PM Motors, Proceedings of the IEEE Energy Conversion Congress and Exposition (ECCE), Milwaukee, USA, September 2016, pp. 1 – 7.

[12] V. Rafiee, J. Faiz: Robust Design of an Outer Rotor Permanent Magnet Motor Through Six-Sigma Methodology Using Response Surface Surrogate Model, IEEE Transactions on Magnetics, Vol. 55, No. 10, October 2019, pp. 1 – 10.

[13] J. Pyrhonen, T. Jokinen, V. Hrabovcova: Design of Rotating Electrical Machines, 2nd Edition, John Wiley & Sons, Inc., Hoboken, New Jersey, 2013.

[14] K. Wang, Z.Q. Zhu, G. Ombach, M. Koch, S. Zhang, J. Xu: Optimal Slot/Pole and Flux-Barrier Layer Number Combinations for Synchronous Reluctance Machines, Proceedings of the 8th International Conference and Exhibition on Ecological Vehicles and Renewable Energies (EVER), Monte Carlo, Monaco, March 2013, pp. 1 – 8.

[15] G. Lei, J. Zhu, Y. Guo, C. Liu, B. Ma: A Review of Design Optimization Methods for Electrical Machines, Energies, Vol. 10, No. 12, December 2017, pp. 1 – 31.

[16] M.J. Kochenderfer, T.A. Wheeler: Algorithms for Optimization, The MIT Press, Cambridge, London, 2019.

[17] G. Lei, J. Zhu, Y. Guo: Multidisciplinary Design Optimization Methods for Electrical Machines and Drive Systems, 1st Edition, Springer, Berlin, 2016.

[18] A. Géron: Hands-On Machine Learning with Scikit-Learn, Keras, and TensorFlow: Concepts, Tools, and Techniques to Build Intelligent Systems, 2nd Edition, O'Reilly Media, Beijing, Boston, 2019.

[19] K. Deb, A. Pratap, S. Agarwal, T. Meyarivan: A Fast and Elitist Multiobjective Genetic Algorithm: NSGA-II, IEEE Transactions on Evolutionary Computation, Vol. 6, No. 2, April 2002, pp. 182 – 197.